8th International IFAC Symposium on
Dynamics and Control of Process Systems
Preprints Vol.1, June 6-8, 2007, Cancún, Mexico

REAL-TIME OPTIMIZATION OF CONTINUOUS PROCESSES VIA CONSTRAINTS ADAPTATION

A. Marchetti, B. Chachuat, and D. Bonvin

Laboratoire d'Automatique
École Polytechnique Fédérale de Lausanne (EPFL)
CH-1015 Lausanne, Switzerland

Abstract: In the framework of process optimization, measurements can be used to compensate for the effect of uncertainty. The method studied in this paper combines a process model and measurements to iteratively improve the operation of continuous processes. Unlike many existing real-time optimization schemes, the measurements are not used to update the process model, but to adapt the constraints in the optimization problem. Upon convergence, all the constraints are respected even in the presence of large model mismatch. Moreover, it is shown that constraints adaptation can handle changes in the set of active constraints. The approach is illustrated, via numerical simulation, for the optimization of a continuous stirred-tank reactor.

Keywords: Static optimization, Constraints adaptation, Measurement-based optimization, Real-time optimization.

1. INTRODUCTION

In the presence of uncertainty, the open-loop implementation of off-line calculated optimal inputs or setpoints leads to suboptimal operation. Worse, the satisfaction of safety constraints and product quality specifications can no longer be guaranteed unless a "conservative" strategy is adopted, i.e., a strategy that ensures constraint satisfaction even in the worst-case scenario (Mönnigmann and Marquardt, 2003; Kang *et al.*, 2004). Unfortunately, this conservatism is detrimental to the optimization objective.

Several measurement-based optimization (MBO) methods have been proposed to deal with uncertainty in the form of model mismatch or process disturbances. For continuous processes, real-time optimization (RTO) attempts to update the operating conditions (e.g., the setpoints), so as to optimize process performance (e.g., its economic productivity). Many successful industrial applications have been reported (Young, 2006).

Typical RTO schemes use measurements for model refinement (Marlin and Hrymak, 1997; Roberts and Williams, 1981), thus implying an iteration between identification and optimization (two-step approach). However, the optimal inputs often fail to provide sufficient excitation for estimating the uncertain parameters accurately. And when sufficient excitation is provided, the resulting solution may no longer be optimal due to the conflicting objectives of parameter estimation and optimization.

Fixed-model methods utilize both the available measurements and a (possibly inaccurate) process model to guide the iterative scheme towards an optimal operating point. Analogous to two-step methods, the available process model is embedded within an NLP problem that is solved repeatedly. But instead of refining the process model from one RTO iteration to the next, the measurements are used to directly update the constraints as well as the cost function in such a way that they approximate the actual cost and constraint functions. The *internal model controller (IMC)*

scheme is one such fixed-model method, wherein the constraint functions are simply offsetted based on their measurements (Desbiens and Shook, 2003). More recently, additional correction terms have been proposed so that, not only the constraint values predicted by the model be equal to those of the actual process constraints, but also their gradients as well as the gradient of the cost function (Gao and Engell, 2005). However, calculating these terms requires that the cost and constraint gradients be estimated from the available measurements.

The focus in this paper is on fixed-model RTO methods, with emphasis on the IMC scheme (Desbiens and Shook, 2003), which we shall refer to as *constraint-adaptation scheme* throughout. The paper undertakes a novel study of various aspects of these adaptation schemes. It is organized as follows. The optimization problem is formulated in § 2. The iterative constraint-adaptation scheme is presented in § 3 and illustrated by a continuous stirred-tank reactor example in § 4. Finally, § 5 concludes the paper.

2. PROBLEM FORMULATION

The usual objective in RTO is the minimization or maximization of some steady-state operating performance of the process (e.g., minimization of the operating cost or maximization of the product rate), while satisfying a number of constraints (e.g., limits on process variables or product specifications), based on a steady-state model of the process. The optimization calculations execute at a given period, and proceed by solving an NLP of the following form:

$$\begin{aligned} \min_{\mathbf{p},\mathbf{x}} \; & J(\mathbf{p},\mathbf{x}) \qquad (1)\\ \text{s.t.} \quad & \mathbf{h}(\mathbf{p},\mathbf{x}) = \mathbf{0} \\ & \mathbf{z}(\mathbf{p},\mathbf{x}) \le \mathbf{z}_{\max} \\ & \mathbf{p}_{\min} \le \mathbf{p} \le \mathbf{p}_{\max}, \end{aligned}$$

where J is a scalar cost function to be minimized, $\mathbf{p} \in \mathbb{R}^{n_p}$ the input (or decision) variables and $\mathbf{x} \in \mathbb{R}^{n_x}$ the state variables. In this formulation, h_i, $i = 1,\ldots,n_x$, stands for the steady-state model of the process, z_i, $i = 1,\ldots,n_z$, is a set of constrained quantities, and $\mathbf{p}_{\min}$, $\mathbf{p}_{\max}$ denote bounds on the input variables (these bounds are considered separately since they are not affected by uncertainty and do not require adaptation).

The necessary conditions of optimality (NCO) for Problem (1) read:

$$\boldsymbol{\mu}^{\mathsf{T}}(\mathbf{z}-\mathbf{z}_{\max}) = 0, \quad \boldsymbol{\mu} \ge \mathbf{0} \qquad (2)$$

$$\boldsymbol{\nu}_+^{\mathsf{T}}(\mathbf{p}-\mathbf{p}_{\max}) = 0, \quad \boldsymbol{\nu}_+ \ge \mathbf{0} \qquad (3)$$

$$\boldsymbol{\nu}_-^{\mathsf{T}}(\mathbf{p}-\mathbf{p}_{\min}) = 0, \quad \boldsymbol{\nu}_- \le \mathbf{0} \qquad (4)$$

$$L_{\mathbf{p}} = \mathbf{0}, \quad L_{\mathbf{x}} = \mathbf{0}, \quad L_{\boldsymbol{\lambda}} = \mathbf{0}, \qquad (5)$$

where $\boldsymbol{\lambda} \in \mathbb{R}^{n_x}$, $\boldsymbol{\mu} \in \mathbb{R}^{n_z}$, $\boldsymbol{\nu}_+, \boldsymbol{\nu}_- \in \mathbb{R}^{n_p}$ are Lagrange multipliers, and L stands for the Lagrangian defined $L = J + \boldsymbol{\lambda}^{\mathsf{T}}\mathbf{h} + \boldsymbol{\mu}^{\mathsf{T}}(\mathbf{z}-\mathbf{z}_{\max}) + \boldsymbol{\nu}_+^{\mathsf{T}}(\mathbf{p}-\mathbf{p}_{\max}) + \boldsymbol{\nu}_-^{\mathsf{T}}(\mathbf{p}-\mathbf{p}_{\min})$. Note that the NCO have two parts: the constraint part (2-4), and the sensitivity part (5).

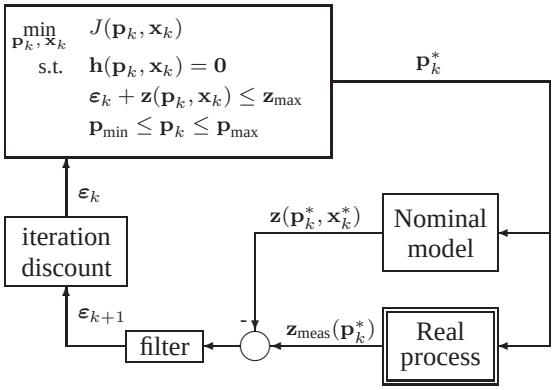

Fig. 1. Iterative constraint-adaptation scheme for static optimization.

3. CONSTRAINT-ADAPTATION SCHEME

The constraint-adaptation scheme is presented in Figure 1. At the k^{th} RTO cycle (or iteration), the NLP problem (1) is solved for $\mathbf{p}_k^*$ and $\mathbf{x}_k^*$ based on the nominal model $\mathbf{h}(\mathbf{p}_k,\mathbf{x}_k) = \mathbf{0}$. Due to model mismatch, the predicted values of the constrained variables, $\mathbf{z}(\mathbf{p}_k^*,\mathbf{x}_k^*)$, do not quite match the measured values $\mathbf{z}_{\text{meas}}(\mathbf{p}_k^*)$. To account for this difference, the corresponding constraints are adapted from cycle to cycle, by using the additive correction terms $\boldsymbol{\varepsilon}_k$. Since the model represents steady-state behavior, great care must be taken that the process has reached steady state before a new input update is made. In other words, the RTO cycle period must be longer than the dynamics of the process.

3.1 Principles of Constraints Adaptation

The constraints in the optimization problem are adapted between successive RTO cycles to track the constraints measured in the real process. This is done by adapting the additive constraint factors $\boldsymbol{\varepsilon}_k$ as follows:

$$\boldsymbol{\varepsilon}_{k+1} = (\mathbf{I}-\mathbf{B})\boldsymbol{\varepsilon}_k + \mathbf{B}(\mathbf{z}_{\text{meas}}(\mathbf{p}_k^*) - \mathbf{z}(\mathbf{p}_k^*,\mathbf{x}_k^*)), \qquad (6)$$

and then considering the modified constraints

$$\boldsymbol{\varepsilon}_k + \mathbf{z}(\mathbf{p}_k,\mathbf{x}_k) \le \mathbf{z}_{\max}, \qquad (7)$$

in the NLP Problem (1). Observe that $\boldsymbol{\varepsilon}_{k+1} \in \mathbb{R}^{n_z}$ is the filtered difference between the measurements $\mathbf{z}_{\text{meas}}(\mathbf{p}_k^*)$ and the model prediction $\mathbf{z}(\mathbf{p}_k^*,\mathbf{x}_k^*)$, both in the previous iteration; $\mathbf{B} \in \mathbb{R}^{n_z \times n_z}$ is a diagonal matrix of filter parameters b_i with $i = 1,\ldots,n_z$. In particular, each constraint can be filtered individually by setting $0 \le b_i \le 1$: no adaptation is performed when $b_i = 0$, whereas no filtering is used when $b_i = 1$.

An important difference with Desbiens and Shook (2003) is that the exponential filtering (6) is performed

on the constraint factors rather than on the inputs. The rationale behind this choice is that it permits to treat each constraint individually. Note also that only the constrained quantities $\mathbf{z}$ are considered for adaptation here, and not the model constraints $\mathbf{h}$. Hence, only the measurements of the constrained quantities $\mathbf{z}$ are required at each RTO cycle.

3.2 Properties of Constraint Adapation

Meeting the Constraints. It is important to ensure that the iterative scheme converges towards the constraints of the real process.

Theorem 1. If the constraint-adaptation scheme converges, then the constraints for the real process are respected.

Proof Upon convergence, i.e., for $k \to \infty$, (6) gives $\boldsymbol{\varepsilon}_\infty = \mathbf{z}_{\text{meas}}(\mathbf{p}^*_\infty) - \mathbf{z}(\mathbf{p}^*_\infty, \mathbf{x}^*_\infty)$. Inserting this equation into (7) leads to $\mathrm{z}_{\text{meas}}(\mathbf{p}^*_\infty) \leq \mathbf{z}_{\max}$. □

It should be noted that the adapatation scheme may converge by following an infeasible path, i.e., with violation of the constraints. This highlights the interest of devising an iterative scheme such that, when starting with initial back-offs from the constraints, the iterations follow a feasible path.

The convergence of the constraint-adaptation scheme can be improved by reducing the performance, i.e, by decreasing the filter parameters b_i. Theoretical conditions under which this scheme converges are not studied in this paper, and will be the topic of future research.

Evaluation of the NCO. With the constraint-adaptation scheme, $\mathbf{z}(\mathbf{p}, \mathbf{x})$ in (1)-(5) specializes to $\boldsymbol{\varepsilon}_k + \mathbf{z}(\mathbf{p}_k, \mathbf{x}_k)$. Upon convergence, and noting that $\boldsymbol{\varepsilon}_\infty + \mathbf{z}(\mathbf{p}^*_\infty, \mathbf{x}^*_\infty) = \mathbf{z}_{\text{meas}}(\mathbf{p}^*_\infty)$, the NCO (2)-(5) can be rewritten as:

$$\boldsymbol{\mu}^{\mathsf{T}}(\mathbf{z}_{\text{meas}}(\mathbf{p}^*_\infty) - \mathbf{z}_{\max}) = 0, \quad \boldsymbol{\mu} \geq \mathbf{0} \tag{8}$$

$$\boldsymbol{\nu}_+^{\mathsf{T}}(\mathbf{p}^*_\infty - \mathbf{p}_{\max}) = 0, \quad \boldsymbol{\nu}_+ \geq \mathbf{0} \tag{9}$$

$$\boldsymbol{\nu}_-^{\mathsf{T}}(\mathbf{p}^*_\infty - \mathbf{p}_{\min}) = 0, \quad \boldsymbol{\nu}_- \leq \mathbf{0} \tag{10}$$

$$L_{\mathbf{p}}|_{\mathbf{p}^*_\infty} = \mathbf{0}, \quad L_{\mathbf{x}}|_{\mathbf{p}^*_\infty} = \mathbf{0}, \quad L_{\boldsymbol{\lambda}}|_{\mathbf{p}^*_\infty} = \mathbf{0} \tag{11}$$

Hence, the constraint part of the NCO (8-10) is determined accurately from the measurements, while the sensitivity part (11) is evaluated using the model, which can be a poor approximation due to model mismatch.

Changing Set of Active Constraints. Much insight on how the method works, and why it can handle changes in the active set, can be gained by visualizing the situation for the simplified problem:

$$\min_{\mathbf{p}} \quad J(\mathbf{p}) \tag{12}$$
$$\text{s.t. } \mathbf{p}_{\min} \leq \mathbf{p}, \quad \varepsilon + z(\mathbf{p}) \leq z_{\max}.$$

In this example, the input $\mathbf{p}$ has two components p_1 and p_2, and there is a single constrained quantity z to be adapted using the constraint factor ε. Figure 2a presents the constrained quantity calculated by the model, $z = z_{\max}$, and the location of the constrained quantity for the real process, $z_{\text{meas}} = z_{\max}$. The shadowed area corresponds to the feasible region of the optimization problem using the model with $\varepsilon = 0$. Point A represents the optimum calculated by the model without constraint adaptation, where the active constraints are $p_{2,\min}$ and $z_{\max}$. However, the optimum of the real process is at point B, where the active constraints are $p_{1,\min}$ and $p_{2,\min}$. In this example, depending on the gradient of the cost $J_{\mathbf{p}}$ calculated with the model, the adaptation may converge to different sets of active constraints. Figure 2b presents the case where, upon adaptation of z, the operation converges to the true optimum B. The shadowed area corresponds to the feasible region of the optimization problem given by the model with $\varepsilon = \varepsilon_B$, where ε_B is evaluated at point B. Figure 2c presents the case where, because of the model mismatch in the evaluation of $J_{\mathbf{p}}$, the adaptation converges to an incorrect set of active constraints at point C. The shadowed area corresponds to the feasible region given by the model with $\varepsilon = \varepsilon_C$, evaluated at point C. The active constraints in this case are $p_{1,\min}$ and $z_{\max}$.

More generally, how close to the true optimum the iterative process gets, and whether or not the correct active constraint set is found, depends upon the error in the estimation of the sensitivities $L_{\mathbf{p}}$ and $L_{\mathbf{x}}$ in (11).

4. ILLUSTRATIVE EXAMPLE

The example presented in Srinivasan *et al.* (2006) is considered to illustrate the constraint-adaptation approach. It consists of an isothermal continuous stirred-tank reactor with two reactions:

$$A + B \longrightarrow C, \qquad 2\,B \longrightarrow D. \tag{13}$$

The desired product is C, while D is undesired. The reactor is fed by two streams with the flow rates F_A and F_B and the corresponding inlet concentrations $c_{A_{in}}$ and $c_{B_{in}}$.

4.1 Model Equations and Parameters

The steady-state model results from material balance equations:

$$F_A c_{A_{in}} - (F_A + F_B)c_A - r_1 V = 0 \tag{14}$$

$$F_B c_{B_{in}} - (F_A + F_B)c_B - r_1 V - 2r_2 V = 0 \tag{15}$$

$$-(F_A + F_B)c_C + r_1 V = 0, \tag{16}$$

with

$$r_1 = k_1 c_A c_B, \qquad r_2 = k_2 c_B^2. \tag{17}$$

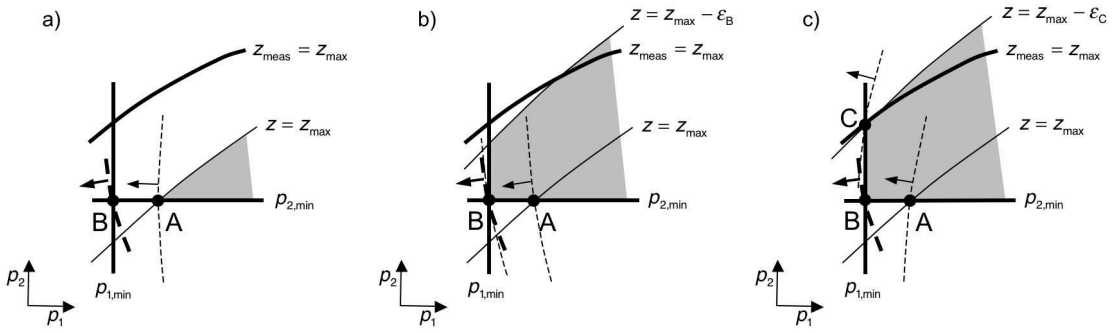

Fig. 2. Sketch of the constraint-adaptation scheme in the 2-D case. Thick solid lines: constraint bounds for the real process. Thin solid lines: constraint bounds evaluated using the model. Thick dashed lines: isoline of J corresponding to the true optimum. Thin dashed lines: isolines of J evaluated using the model. Arrows: negative of the cost gradient, $-J_{\mathbf{p}}$. a) No constraint adaptation. Point A: Nominal model optimum; Point B: Real process optimum. b) Constraint adaptation and convergence to the true optimum B. c) Constraint adaptation and convergence to the suboptimal solution C.

The heat produced by the chemical reactions is:

$$q_r = (-\Delta H_1) r_1 V + (-\Delta H_2) r_2 V. \qquad (18)$$

Variables and parameters: c_X: concentration of species X, V: volume, r_i: rate of reaction i, k_i: kinetic coefficient of reaction i, ΔH_i: enthalpy of reaction i.

Table 1. Nominal model parameters and operating bounds

$k_{1,\text{nom}}$	1.5	$\frac{\text{l}}{\text{mol h}}$	k_2	0.014	$\frac{\text{l}}{\text{mol h}}$
$c_{A_{in}}$	2	$\frac{\text{mol}}{\text{l}}$	$c_{B_{in}}$	1.5	$\frac{\text{mol}}{\text{l}}$
ΔH_1	-7×10^4	$\frac{\text{J}}{\text{mol}}$	ΔH_2	-10^5	$\frac{\text{J}}{\text{mol}}$
V	500	l	$q_{r,\max}$	10^6	$\frac{\text{J}}{\text{h}}$
$F_{\max}$	22	$\frac{\text{l}}{\text{h}}$			

The numerical values of the parameters are given in Table 1. Since, in this work, the reality is simulated by varying k_1 in the model, the nominal value of k_1 is denoted by $k_{1,\text{nom}}$. Note that this value is different from the one used in Srinivasan *et al.* (2006).

4.2 Optimization Problem

The cost function is chosen as the amount of product C, $(F_A + F_B)c_C$, multiplied by the yield factor $(F_A + F_B)c_C / F_A c_{A_{in}}$. Upper bounds are defined for the amount of heat produced by the reactions and the total flow (Table 1). The optimization can be formulated mathematically as:

$$\begin{aligned} \max_{F_A, F_B} \quad & J = \frac{(F_A + F_B)^2 c_C^2}{F_A c_{A_{in}}} \qquad (19) \\ \text{s.t.} \quad & \text{model equations (14)-(18)} \\ & F_A + F_B \le F_{\max} \\ & q_r \le q_{r,\max}. \end{aligned}$$

The optimal feed rates, the values of the constrained quantities, and the cost function for $k_1 = 0.3$, 0.75 and 1.5 $\frac{\text{l}}{\text{mol h}}$ are given in Table 2. Notice that the set of active constraints in the optimal solution changes with the value of k_1.

Table 2. Optimal solutions for various values of the parameter k_1

k_1	F_A^*	F_B^*	$\frac{q_r}{q_{r,\max}}$	$\frac{F_A+F_B}{F_{\max}}$	Cost
0.3	8.21	13.79	0.887	1.000	8.05
0.75	8.17	13.83	1.000	1.000	11.16
1.5	7.61	13.05	1.000	0.940	12.30

4.3 Iterative Constraints Adaptation

Since the constraint on $(F_A + F_B)$ is not affected by the uncertainty, only the constraint on q_r requires adaptation.

4.3.1. Accuracy of the Constraint-Adaptation Scheme

In this subsection, the accuracy of the constraint-adaptation scheme upon convergence is investigated in the absence of measurement noise and process disturbances (ideal case).

The scaled constrained quantities $q_r/q_{r,\max}$ and $(F_A + F_B)/F_{\max}$ are represented in Figure 3 for values of k_1 (simulated reality) varying in the range 0.3 to 1.5 $\frac{\text{l}}{\text{mol h}}$. Note that the constrained quantities obtained with the the constraint-adaptation scheme (thick lines) follow closely those of the true optimal solution (thin lines). However, although the proposed scheme guarantees feasible operation upon convergence irrespective of the value of k_1, it fails to detect the correct active set in the vicinity of the operating points where the active set changes (i.e., $k_1 \approx 0.65$ and $k_1 \approx 0.8$). As discussed in subsection 3.2, this deficiency results from the error introduced by the nominal model in the evaluation of the sensitivities with respect to F_A and F_B of both the cost function and the state constraints.

Figure 4 shows the performance loss

$$\Delta J := \frac{J_{\text{true}} - J(\mathbf{p}_\infty^*, \mathbf{x}_\infty^*)}{J_{\text{true}}},$$

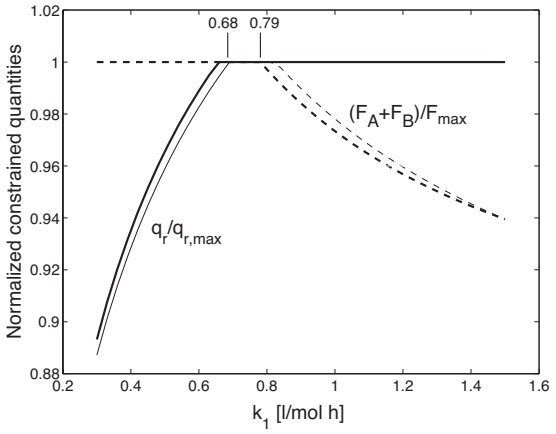

Fig. 3. Optimal values of the constrained quantities $q_r/q_{r,\max}$ and $(F_A + F_B)/F_{\max}$ versus k_1, for $k_{1,\text{nom}}$ = 1.5 $\frac{\text{l}}{\text{mol h}}$. Thick lines: Constraint-adaptation solution; Thin lines: True optimal solution.

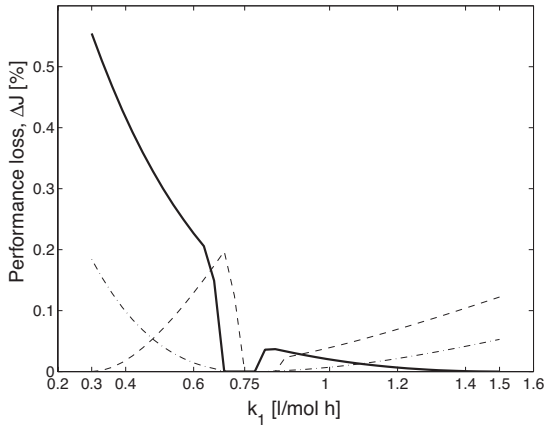

Fig. 4. Performance loss of the constraint-adaptation solution. Thick line: $k_{1,\text{nom}}$ = 1.5 $\frac{\text{l}}{\text{mol h}}$; Thin dot-dashed line: $k_{1,\text{nom}}$ = 0.75 $\frac{\text{l}}{\text{mol h}}$; Thin dashed line: $k_{1,\text{nom}}$ = 0.3 $\frac{\text{l}}{\text{mol h}}$.

where J_{true} denotes the true optimal cost, and $J(\mathbf{p}^*_\infty, \mathbf{x}^*_\infty)$ the optimal cost obtained upon convergence of the constraint-adaptation scheme. Clearly, ΔJ is equal to zero for k_1 = 1.5, for there is no model mismatch in this case. Interestingly enough, ΔJ is also equal to zero when the two constraints are active and the adaptation scheme provides the correct active set; this situation occurs for k_1 in the range $0.68 < k_1 < 0.79$ (see Figure 3). Overall, the performance loss remains lower than 0.6% for any value of k_1 in the range 0.3 to 1.5 $\frac{\text{l}}{\text{mol h}}$, and is even lower (less than 0.2%) with $k_{1,\text{nom}}$ chosen as 0.3 and 0.75 $\frac{\text{l}}{\text{mol h}}$ in the nominal model. These results demonstrate that the performance loss remains limited, despite the error made in the detection of the active set for some scenarios.

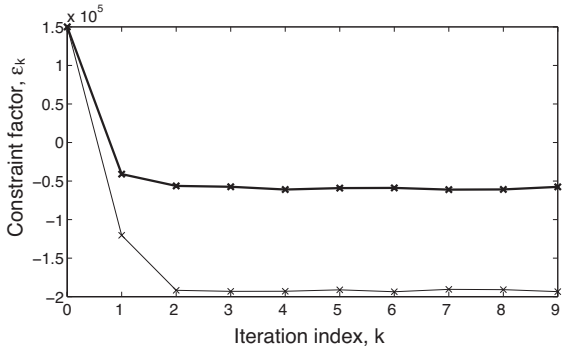

Fig. 5. Evolution of the constraint factor ε. Thick line: Case 1; Thin line: Case 2.

4.3.2. Convergence of the Constraint-Adaptation Scheme In this subsection, we take a closer look at the convergence properties of the iterative scheme. Two scenarios are considered, which correspond to different sets of active constraints at the optimum. In either scenario, the nominal model is chosen with $k_{1,\text{nom}}$ = 1.5 $\frac{\text{l}}{\text{mol h}}$. Note also that the adaptation is started with a highly conservative initial constraint factor $\varepsilon_0 = 1.5 \times 10^5$ $\frac{\text{J}}{\text{h}}$, and the filter parameter is taken as $b = 1$ (no filtering).

To depart from the ideal case of the previous subsection, Gaussian noise with standard deviation of 1800 $\frac{\text{J}}{\text{h}}$ is added to the measurements of q_r. In response to this, a back-off is defined to ensure that the heat production constraints is satisfied, i.e., $q_{r,\max} = 9.9 \times 10^5$ $\frac{\text{J}}{\text{h}}$.

Case 1) Simulated Reality with $k_1 = 0.75$. The evolution of the constraint factor ε with the RTO cycle is shown in Figure 5 (thick line). A negative value of ε indicates that the heat production is overestimated by the model, which is consistent with the values of k_1 chosen for the simulated reality. Note also that the convergence is very fast in this case, as the region where the adaptation is within the noise level is reached after two RTO cycles only. The corresponding constrained quantities $F = F_A + F_B$ and q_r are represented in Figure 6. Observe that only the heat production constraint is active in this scenario, and that the chosen back-off ensures that the maximum value of 10^6 $\frac{\text{J}}{\text{h}}$ does not get exceeded despite measurement noise. On the other hand, the feed rate constraint remains inactive, although its value gets close to the maximum feed rate. Finally, the evolution of the cost function J is shown in Figure 7 (thick line). The converged cost value is close to 11, i.e., within a few percent of the ideal cost given in Table 2, despite the performance loss induced by backing-off the heat production constraint.

Case 2) Simulated Reality with $k_1 = 0.3$. The evolution of the constraint factor ε, the constrained quantities $F = F_A + F_B$ and q_r, and the objective function J is shown as thin lines in Figures 5, 6 and 7, respectively. It is seen from Figure 5 that the constraint factor is larger in this scenario than in the previous one, as

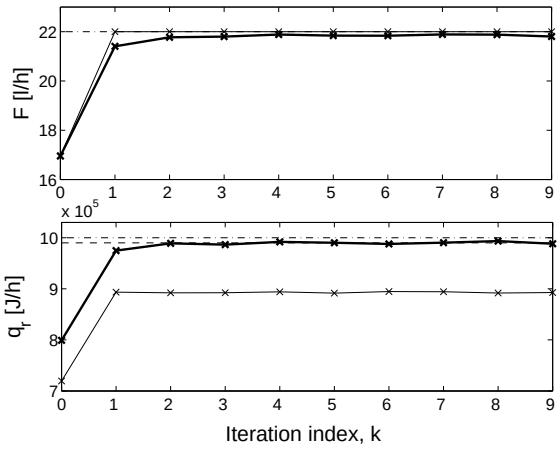

Fig. 6. Evolution of the constrained quantities. Thick lines: Case 1; Thin lines: Case 2.

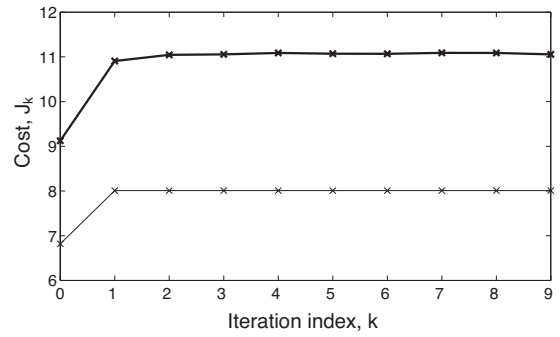

Fig. 7. Evolution of cost function. Thick lines: Case 1; Thin lines: Case 2.

the nominal model is even farther from the simulated reality. Moreover, Figure 6 shows that only the feed rate constraint gets active, while the heat production remains inactive. Hence, the optimal inputs remain unaffected by measurement noise. It takes a single RTO cycle for the constraint-adaptation scheme to detect the correct active set in this case. Finally, it is seen from Figure 7 that the converged cost value of about 8 is very close to the ideal cost reported in Table 2, in spite of the large model mismatch.

5. CONCLUSIONS

In this paper, a constraint-adaptation scheme has been applied to the context of RTO. The input variables are updated at each RTO cycle, based on a (nominal) process model, by solving a constrained NLP problem. Only the state constraints of the optimization problem are adapted, based on the measured constrained quantities. Constraint satisfaction is guaranteed upon convergence. When the optimal solution lies on the constraints of the optimization problem, the constraint-adaptation scheme pushes the operation towards the constraints of the real process. Thus, the method is especially well suited to those optimization problems where meeting the active constraints has a dominant impact on the cost. In those cases, near optimality can be obtained within a small number of iterations, even in the presence of (considerable) model mismatch.

A major advantage with respect to many existing RTO methods is that the nominal model does not require refinement, and thus the conflict between the parameter estimation and optimization objectives is avoided. This feature, together with constraint satisfaction and fast convergence, makes the constraint-adaptation approach much appealing for RTO applications.

This paper has demonstrated that the constraint-adaptation approach has the ability to capture changes in the set of active constraints. The NCO-tracking scheme (Srinivasan *et al.*, 2003) uses measurements and feedback control to enforce the NCO for the true process, but it relies on the assumption that the active set does not change with uncertainty. Hence, both approaches could complement each other nicely, and finding a proper way of doing so will be the topic of future work.

REFERENCES

Desbiens, A. and A. A. Shook (2003). IMC-optimization of a direct reduced iron phenomenological simulator. In: *4th International Conference on Control and Automation*. Montreal, Canada. pp. 446–450.

Gao, W. and S. Engell (2005). Iterative set-point optimization of batch chromatography. *Comp. Chem. Eng.* **29**, 1401–1409.

Kang, J. S., M. H. Suh and T. Y. Lee (2004). Robust economic optimization of process design under uncertainty. *Eng. Optim.* **36**(1), 51–75.

Marlin, T. E. and A. N. Hrymak (1997). Real-time operations optimization of continuous processes. In: *American Institute of Chemical Engineering Symposium Series - Fifth International Conference on Chemical Process Control*. Vol. 93. pp. 156–164.

Mönnigmann, M. and W. Marquardt (2003). Steady-state process optimization with guaranteed robust stability and feasibility. *AIChE J.* **49**(12), 3110–3126.

Roberts, P. D. and T. W. Williams (1981). On an algorithm for combined system optimisation and parameter estimation. *Automatica* **17**(1), 199–209.

Srinivasan, B., D. Bonvin, E. Visser and S. Palanki (2003). Dynamic optimization of batch processes: II. Role of measurements in handling uncertainty. *Comp. Chem. Eng.* **27**, 27–44.

Srinivasan, B., L. T. Biegler and D. Bonvin (2006). Tracking the necessary conditions of optimality with changing set of active constraints using a barrier-penalty function. *Comp. Chem. Eng.* submitted.

Young, R. E. (2006). Petroleum refining process control and real-time optimization. *IEEE Contr. Syst. Mag.* **26**(6), 73–83.